

Parton Distribution Functions and Amplitudes of the Pseudoscalar Mesons and the Nucleon from Lattice QCD

Robert Edwards, Christos Kallidonis, Nikhil Karthik, Jianwei Qiu,

David Richards*, Eloy Romero, Frank Winter

Jefferson Lab

Balint Joo

ORNL

Carl Carlson, Chris Chamness, Colin Egerer, Tanjib Khan, Daniel Kovner,

Christopher Monahan, Kostas Orginos, Raza Sufian

College of William and Mary

Wayne Morris, Anatoly Radyushkin

Old Dominion University

Joe Karpie

Columbia University

Savvas Zafeiropoulos

Aix Marseille Univ, Marseille, France

Yan-Qing Ma

Peking University, Beijing, China

March 8, 2021

Abstract

A long-standing challenge in lattice QCD is the direct computation of key measures of hadron structure, including parton distribution functions, quark distribution amplitudes, and three-dimensional measures such as the transverse-momentum-dependent distributions, and generalized parton distributions. Recently, new approaches have been proposed that enable their direct computation, and these are characterized by a requirement that the hadron of interest be increasingly relativistic. This **Class A Continuation** proposal aims to capitalize on recent developments, and our previous USQCD allocation, to compute the structure functions of the pion and nucleon using the pseudo-PDF formulation using the distillation framework, to extend the calculation to that of the gluon contribution to hadron structure, and to embark on calculations of three-dimensional imaging through the calculation of GPDs in the pseudo-PDF approach. This project is relevant to the hadron structure experimental programs at JLab, and at RHIC-spin. With the recent CD0 and site selection of the EIC, the extension to the gluon distributions and the study of pion and kaon physics is particularly timely. **We request an allocation of 43.5 KNL-core-hours, 0.78M GeForge GPU-Hours, 7.43M SKX-core-hours, together with an addition 100 TByte tape storage, and 60 Tbyte of disk storage.**

*email: dgr@jlab.org

1 Goals and Milestones

Nuclear physics is a vast, rich field, whose phenomenology has been explored for decades through intense experimental and theoretical efforts. However, it is only now that direct connections to quantum chromodynamics (QCD), the underlying theory of the strong interactions, and the basic building blocks of nature, quarks and gluons, are solidifying. The phenomena of confinement and chiral symmetry breaking are jointly responsible for the intervening forty years of research and development between the discovery of QCD [1, 2, 3], the formulation of QCD on a discretized space-time [4] and recent numerical solutions of simple systems at the physical values of the quark masses along with the inclusion of electromagnetism. This new-found ability is changing nuclear physics. It is permitting us to address key questions that define the field, such as how the observed particles emerge from QCD, how gluons manifest themselves in the spectrum and structure of hadrons, and how the spin and other attributes of the pion and proton are partitioned between the quarks and gluons. The target for this proposal is to refine critical aspects of the nature of strongly interacting particles composed of quarks and gluons and their dynamics by direct calculations at the physical light quarks masses using the numerical technique of lattice QCD.

One of the great challenges posed by QCD is to understand how protons and neutrons, the basic building blocks of most of the observed matter in the universe, are made from quarks and glue. First principles calculations in this area are directly relevant to the experimental programs at JLab 12 GeV and LHC, and the future electron-ion collider (EIC), to be sited at BNL and which has now received CD0. Our knowledge of hadron structure is encapsulated in a variety of measures. From the earliest observations of Bjorken scaling in Deep Inelastic Scattering, a one-dimensional longitudinal description of the nucleon has been provided through the unpolarized and polarized *Parton Distribution Functions* (PDFs). In contrast, the transverse distribution of charge and currents was probed in elastic scattering, encapsulated in the electric and magnetic form factors. More recently, new measures have been discovered correlating both the longitudinal and transverse structures: the *Generalized Parton Distributions* (GPDs) describing hadrons in longitudinal fractional momentum x and impact-parameter space, and the *Transverse-Momentum-Dependent Distributions* (TMDs) providing a description in x and transverse momentum space. These new descriptions have opened new vistas on the nucleon, in particular enabling orbital angular momenta to be discerned.

From the inception of these new measures, the lattice community has attempted to calculate them from first principles. However, the formulation of lattice QCD in Euclidean space provides a formidable restriction: the x dependence could not be computed directly, but only the x moments of the distributions. Furthermore, the breaking of rotational symmetry on the lattice in practice restricted such calculations to only the first few moments. Recently, new ideas have been proposed that aim to circumvent one or more of these restrictions[5, 6, 7, 8, 9, 10, 11, 12].

The work proposed here will be to further exploit these new methods to investigate the properties of the pion, the lightest hadron composed of the light u , and d , and of the nucleon through calculation of so-called good “Lattice Cross Sections” identified in ref. [12], and through the calculation of pseudo-PDFs[11]. In particular, we will calculate the collinear one-dimensional x -dependent parton distribution function of the pion and nucleon, notably at large x . The calculations proposed here can also be used to compute the moments of the parton distributions for comparison with earlier works [13].

The determination of large- x part of the pion PDF is the goal of the approved experiment C12-15-006 at Jefferson Lab, whilst the determination of the kaon structure function is the goal of the approved run-group C12-15-006A. Furthermore, the approved experiments E-03-012, E-00-002, at Jefferson Lab (12 GeV) are targeting the determination of the nucleon structure functions at large- x . The large- x region is precisely the region our computational methods are more effective and therefore

Ensemble ID	a (fm)	M_π (MeV)	β	$L^3 \times T$
E1	0.094(1)	390(3)	6.3	$32^3 \times 64$
E2	0.094(1)	270(3)	6.3	$32^3 \times 64$
E3	0.091(1)	170(2)	6.3	$48^3 \times 96$
E4	0.0728(8)	272(3)	6.5	$48^3 \times 128$

Table 1: Table of Wilson-clover lattices referenced in this proposal.

our work is in close synergy with the already approved experimental efforts at Jefferson Lab. In addition to the experimental program at Jefferson Lab, at the Theory Center, the JAM collaboration aims towards the determination of PDFs from experimental data. Our future plans include a close collaboration with JAM using our lattice QCD results to further enhance the fidelity of the pion and nucleon PDFs.

Our proposed program of work for the coming year capitalizes on the progress during the current allocation period in both computational efficiency and physics reach. Firstly, we have clearly shown the advantage of the distillation framework for the calculation of hadron structure using the pseudo-PDF approach; we will exploit this to refine our current calculations of the parton distribution functions of the nucleon and pion, and to calculate at near-to-physical light-quark masses. Secondly, we will use the high statistical precision and sampling of the gauge configurations facilitated through the use of distillation to perform calculations of the gluon contributions to nucleon structure. Finally, we will take advantage of computational efficiencies over the current allocation period to advance our studies of GPDs within the pseudo-PDF framework.

The framework for the calculation of Bjorken- x -dependent PDFs using the pseudo-PDF and “lattice cross section” approaches has been described in the introduction to our 2019 proposal. We will not repeat that description here. However, we note that both the pseudo-PDF and quasi-PDF frameworks involve the computation of the same matrix elements, e.g. a quark and anti-quark separated by a Wilson line, with different renormalization prescriptions. Both the pseudo-PDF and LCS approaches provide a framework that permits collinear factorization with a well-defined short-distance scale z^2 , and are expressed in terms of Lorentz invariants, the Ioffe time and z^2 .

Progress since last USQCD Submission

Nucleon PDF at the physical quark mass

We have extended the calculation of the unpolarized nucleon PDF reported last year to provide a calculation of the nucleon PDF at physical pion mass[14], through the inclusion of the close-to-physical E3 ensemble of Table 1. This is the first such study employing the method of Ioffe-time pseudo-distributions. We show our results, together with related computations, in Figure 1.

An important part of our strategy is finding an efficient means of relating the matrix elements computed on the lattice to the PDFs and other key measures of hadron structure. In ref. [15], some members of this project team analysed our lattice within the NNPDF framework to obtain two non-singlet parton distribution functions.

Distillation at High Momentum and Parton Distribution Functions

An important requirement for precise calculations of hadron structure is a sufficient range in the Ioffe time $\nu = p \cdot \xi$, where p and ξ are the hadron momentum and spatial separation, respectively,

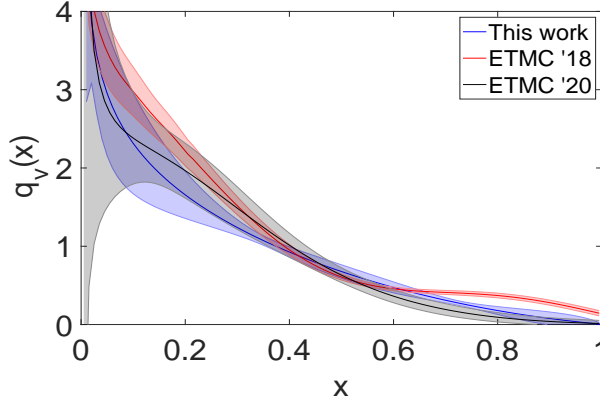


Figure 1: Our determination of the nucleon light-cone PDF at the physical pion mass, compared to the 2018 results of ETMC employing the method of quasi-PDFs and compared to the 2020 results of ETMC which is a re-analysis of the same lattice data albeit with the method of pseudo-PDFs.

thereby requiring that we be able to boost the hadron to high momentum. Unfortunately, the signal-to-noise ratio rapidly degrades at large momentum, and the contamination by excited states more severe, both through the reduced symmetry for states in motion, and through the compression of the gap energy gap between the lowest-lying energy and those of the excitations. We have developed a new approach[16] whereby we combine distillation[17] with so-called “momentum smearing”[18]. The success of this method in resolving the nucleon at high spatial momenta is illustrated in Figure 2, where we show the dispersion relation for the nucleon using the straightforward implementation of distillation, together with the amalgam of distillation and momentum smearing, denoted by “phasing”. Having established our ability to reach high momentum for the nucleon through the dispersion

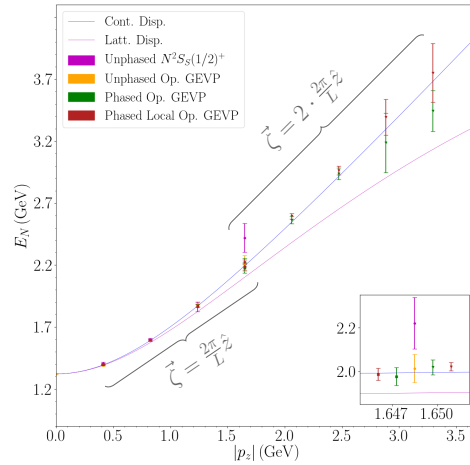


Figure 2: The ground-state nucleon dispersion relation for the nucleon at a pion mass of around 360 MeV, together with expectations from the continuum dispersion relation (blue), and free lattice dispersion relation (purple). “Vanilla” distillation for a single interpolating operators $N^2 S_2^{1/2+}$, and using the variational method with a basis of operators, are shown in magenta and orange, respectively. Using “phasing” and the variational method with a basis of local operators, and extended operators, are shown in red and green, respectively; ζ denotes the phasing factor.

relation, we now proceed to look at the ability to compute nucleon matrix elements, focusing on the various nucleon charges for states in motion. This is illustrated for the case of the renormalized tensor charge in Figure 3.

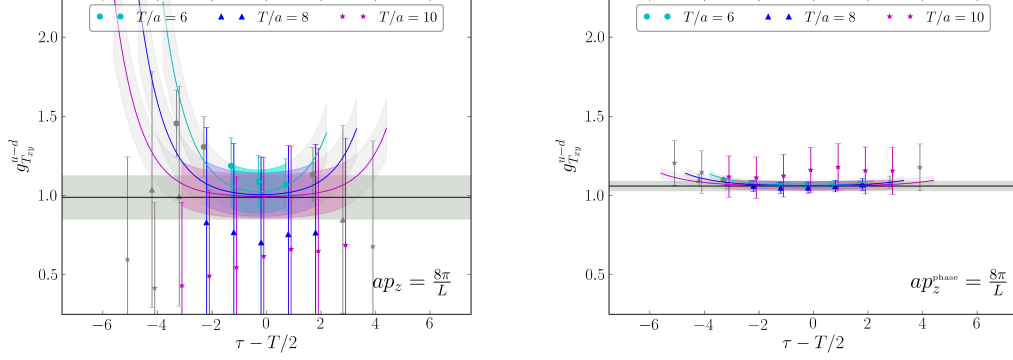


Figure 3: The left- and right-hand plots show the effective renormalized tensor charge g_T at several separations T between the source and sink nucleons for a nucleon with momentum $ap_z = 8\pi/L$ without phasing, and with two units of phasing, respectively[16].

We are currently exploiting our momentum-smeared implementation of distillation to compute the nucleon PDF to high precision, and we show preliminary results in Fig. 4. Compared to previous work that employed the same ensemble E1[19], these results demonstrate very significant improvement both in the reach in ITD, and in the statistical uncertainties; this work is currently being prepared for publication.

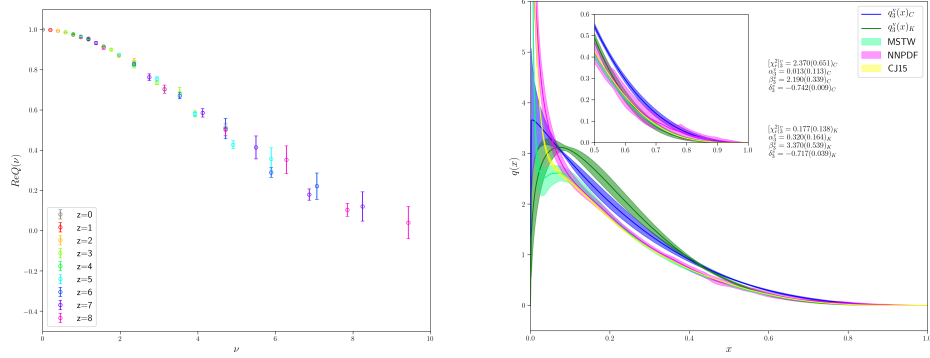


Figure 4: The left-hand plot shows the real part of the Ioffe-Time distribution on the ensemble E1 of Table 1. The right-hand plot shows the corresponding PDF; C and K to denote two different approaches to relating the ITD to the PDF. Also shown are analyses from global fits to experimental data (MSTW, NNPDF, CJ15).

Unpolarized Gluon Distribution

We apply the reduced pseudo PDF approach, proposed in [9] and applied to the gluon case in [20], to obtain a renormalization-group-invariant distribution. We apply the gradient flow, which significantly reduces short-range fluctuations that contribute to the signal-to-noise challenges, to improve the signal-to-noise ratio. Moreover, the flow provides a mechanism to understand the spatial dependence

of our results in a continuous manner. Preliminary results for the unpolarized ITD at two values of the flow time τ are shown in Figure 5. One member of our team has investigated the implications of parametrizations of the polarized and unpolarized gluon distributions for the gluon ITD that can be computed on the lattice[21], which might provide important additional phenomenological input to our lattice calculations given the limited range of Ioffe times are accessible.

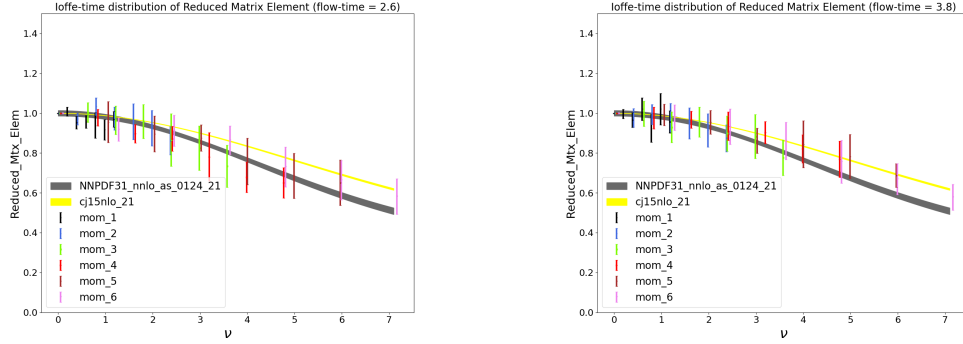


Figure 5: The left-and right-hand plots show the preliminary results for the unpolarized reduced gluonic matrix element vs the Ioffe time ν , for flow times 2.4 and 3.8 respectively, obtained on the ensemble E1. Also shown are expectations from global fits.

Work Plan for 2021-2022 Allocation Year

Our work this year focuses on three topics: flavor-singlet nucleon structure, three-dimensional nucleon structure encapsulated in the Generalized Parton Distributions, and the structure of the kaon and pion. We will maintain our program of performing our calculations within the pseudo-PDF framework as distributions in (pseudo-) Ioffe Time.

PROJECT I: Flavor-singlet hadron structure

The extension of our work to include the flavor-singlet nucleon structure requires both the computation of the disconnected diagrams, and the contributions of the matrix elements of the gluonic operators with which they mix, using the gradient-flow method to renormalize the resulting matrix elements. One outcome of our work over the last year has been the need for very high level of statistics to attain the quality of the data presented in Figure 5 which is reflected in the request below.

PROJECT II: Three-Dimensional Nucleon Structure

We will continue our study of the one- and three-dimensional structure of the nucleon, encapsulated in the PDF and GPDs, respectively. As we discuss below, we have made considerable improvements to our code which enables us to study a broad range of matrix elements, including those for the polarized and unpolarized PDF, for the transversity distributions, and notably for the polarized and unpolarized GPDs. In our last submission, we were only able to propose computations of GPDs on one ensemble, and for a very limited range of momentum transfers. With our recent improvement to the code base, we are now able to study a broad range of physics on each ensemble, and furthermore for all possible Dirac structures at the operator.

1.1 PROJECT III: Properties of the Pion and Kaon

The pion and kaon play a seminal role in QCD in being the close-to-Goldstone bosons of the theory, and understanding their nature goes to the heart of the origin of mass. This importance is reflected in the flagship role of proposed pion and kaon experiments at the EIC, articulated in a recent review to which members of our team contributed[22], and to other experiments worldwide, including at COMPASS at CERN. Our work this year will focus both on the pion and kaon PDFs, and also on the quark distribution amplitudes (DA's) relevant to the behavior of exclusive process at high momentum transfers.

Computational Strategy

Our strategy will be to use an already generated gauge ensembles, with a clover-fermion action, lattice spacings $a \simeq 0.09$ and 0.072 fm, with pion masses down to 170 MeV. The framework for our calculations will be *distillation*, which was described in detail in our 2019-2020 proposal. Thus we will only outline the salient points of the method for our program of calculations in this document.

In summary, distillation is a method of smearing in which the smearing $\square(t)$ is expressed as a truncated outer product of eigenvectors $v^{(i)}(t)$ of the three-dimensional Laplacian

$$\square(t) = \sum_{i=1}^{N_{\text{vec}}} v^{(i)}(t) v^{(i)\dagger}(t). \quad (1)$$

For compactness, we will discuss the case of mesons, where we write a “smeared” two-point correlation function as

$$C_{AB}(t_f, t_i; \vec{p}) = \text{Tr} \langle \Phi^A(\vec{p}, t_f) \tau(t_f, t_i) \Phi^B(\vec{p}, t_i) \tau^\dagger(t_f, t_i) \rangle \quad (2)$$

where

$$\Phi_{\alpha\beta}^{A,ij}(\vec{p}, t) = \sum_{\vec{x}} v^{*(i)}(\vec{x}, t) e^{-i\vec{p}\cdot\vec{x}} [\Gamma^A(t) \gamma_5]_{\alpha\beta} v^{(j)}(\vec{x}, t) \quad (3)$$

$$\tau_{\alpha\beta}^{ij}(t_f, t_i) = v^{*(i)}(t_f) M_{\alpha\beta}^{-1}(t_f, t_i) v^{(j)}(t_i). \quad (4)$$

Here $i, j = 1, \dots, N_{\text{vec}}$, α, β are spinor indices, and t_i, t_f the source and sink timeslices respectively, and Γ is an operator that may include derivatives. The crucial observation in the above construction is that the Φ 's of eqn. 3, denoted “elementals”, encode the structure of the operator, with, for example, derivatives now acting on the (quark-mass-independent) ξ 's, whilst the parallel transport of the quark fields is encoded in the “perambulators” of eqn. 4. The advantages of the method are three-fold. Firstly, the factorization between the perambulators and elementals enables operators of essentially unrestricted spatial structure to be used at both source and sink, without the calculation of additional perambulators. Secondly, correlator of eqn. 2 involves spatial sums both at the source and at the sink, thus providing a more complete sampling of the lattice. Finally, the form of eqn. 2 can straightforwardly be extended to baryons, with only the need for the calculation of an appropriate set of baryon “elementals”. The implementation of momentum smearing within the distillation framework requires the computation of boosted perambulators, obtained from the boosted eigenvectors

$$\tilde{v}^{(i)}(\vec{x}, t) = e^{i\vec{\zeta}\cdot\vec{x}} v^{(i)}(\vec{x}, t) \quad (5)$$

where $\vec{\zeta}$ is a three-momentum allowed on our lattice.

The calculation of three-point functions proceeds likewise, and it involves the introduction of so-called “generalized perambulators”, denoted by *genprop* below. The *genprop* between the source time t_i and the sink time t_f have the structure

$$J^{ij}(t_f, t, t_i) = v^{(i)\dagger}(t_f) M^{-1}(t_f, t) \Gamma(t) \mathcal{D} \mathcal{P} M^{-1}(t, t_i) v^{(j)}(t_i) \quad (6)$$

where Γ is a spin matrix, \mathcal{D} is a Wilson line, \mathcal{P} is a momentum projector and, t is varying in the interval (t_f, t_i) . The resulting three-point function can then be written

$$C_{AB}^{3\text{pt}}(t_f, t_i, t; x_0, \xi, \vec{p}) = \text{Tr} \langle \phi^A(\vec{p}, t_f) J(t_f, t, t_i) \Phi^B(\vec{p}, t) \tau^\dagger(t_f, t_i) \rangle, \quad (7)$$

for the case of mesons. $C_{AB}^{3\text{pt}}$ is of the same form as C_{AB} of eqn. 2, with one of the perambulators replaced by a generalized perambulator. Note that in the pseudo-PDF calculation of eqn ??, there is an additional time-sliced sum at t . This has two important consequences. Firstly, for the pseudo-PDF calculation of the nucleon, we are able to perform momentum projections at each time location in a three-point function, something we have not been able to achieve using our previous methods. Secondly, the ability to insert momentum at t enables us to explicitly introduce a momentum transfer thus facilitating the calculations of the off-forward matrix elements describing GPDs. Note the same set of *perambulators* and *generalized perambulators* are employed for baryon and meson structure calculations.

Software

We will use the *Chroma* software framework, which now supports multigrid on the GPUs, KNLs and the Skylake nodes. For the computation of the elements, we use *harom*, running on top of the three-dimensional *qdp++* code. Finally, we use *redstar* for the contraction of the perambulators, generalized perambulators and elementals to form the correlation functions of eqn. 2 and 7.

We construct the *genprops* needed for our correlation functions with a newly developed software that computes quark propagators and contract them in one task, avoiding the large I/O of storing the quark propagators. The calculation of the sink and source tensors,

$$T_{\text{sink}}^{(i)} = v^{(i)\dagger}(t_f) M^{-1}(t_f, t) \quad T_{\text{src}}^{(i)} = M^{-1}(t, t_i) V^{(i)}(t_i),$$

involves the inversion of M , the lattice Dirac operator, and uses program code for high-performance and advanced algorithmic inversion of the fermion matrix, which relies on a lattice grid that uses a four-dimensional space-time layout. This part of the calculation runs in capacity mode and utilizes all compute nodes within the job, where each node processes a four-dimensional sub-grid of the lattice. The correlation length t varies only over a sub-domain of the full time-extent of the lattice, so we are interested in computing the contraction of T_{sink} and $\Gamma(t) \mathcal{D} \mathcal{P} T_{\text{src}}$ on this sub-domain only. However, because of the way the data is arranged, only a small portion of the computing nodes will participate in the computation, dramatically impacting the overall performance of generating *genprops*. The new code reduces by an order of magnitude the time expended in contractions by redistributing the data to balance the computation among the nodes, and rearranging the contractions as dense matrix-matrix multiplications, which are done with an optimized BLAS.

Resource Request

PROJECT I: Flavor-singlet hadron structure

This computation of the gluonic matrix elements involves only the calculation of the two-point nucleon correlators, the computation of any gluonic operators being negligible. As discussed earlier, the

computation of the gluonic matrix elements is subject in particular challenges in obtaining the needed signal-to-noise ratios. We will therefore focus on a calculation on a single ensemble, namely E4 of Table 1, and compute the needed perambulators from every other time slice on our lattice, and compute them on a further 600 configurations beyond those employed for the isovector studies below. During the past year, we have developed an effective strategy wherein the perambulators are computed on the "gaming" GPU nodes at Jefferson Lab, whilst the baryon elementals, which are not stored, and the computations of the resulting matrix elements are computed on the Skylake nodes at FNAL; the requested resources in the first panel of Table 2 are obtained from the observed times for the calculation on the ensemble E1.

For the computation of the disconnected diagram, we have recently developed [23] methodologies that rely on AAMG deflation as well state-of-the-art probing methods [24] to reduce by orders-of-magnitude the variance of the stochastic estimator. Our timings are obtained using the observed solver times on the target lattice on the KNL at Jefferson Lab.

Ens	Res	Task	Soln (g-s)	N_D	N_{t_i}	N_b	N_{inv}	g/c-h/Cfg	N_{cfg}	Tot (g/c-h)
E4	RTX	Peram	6.3	96	48	5	92,160	1,296	600	778K
	SKX	Elem/2pt						12,380	600	7,428K
	Ens	Res	Task	Soln (c-s)	$N_{\text{inv,d}}$	$N_{\text{inv,p}}$	c-h/Cfg	N_{cnf}	Tot (c-h)	
	E4	KNL	Disco	2048	21,600	1536	26,324	600	13,162K	

Table 2: The upper table shows the cost of computing the gluon matrix elements, where N_D is the rank of the distillation space, N_b is the total number of boosts ($0, \pm 1, \pm 2$), N_{inv} is the total number of inversions per configuration, and N_{cfg} is the number of configurations. The lower table shows the cost of computing the disconnected diagrams in KNL core-hours, where $N_{\text{inv,d}}$ is the number of inversions for the distillation vector, $N_{\text{inv,p}}$ is the number of inversions for the probing vectors. In each case, Soln denotes the cost of a solution in GPU- or node-seconds; for the disconnected diagrams, the cost of inserting the matrix elements increases the cost by a factor of two, reflected in the table. The total cost on the respective resource is shown in the final column as GPU-hours (RTX) or core-hours (SKX and KNL) as appropriate.

PROJECT II: Three-dimensional Nucleon Structure

As we note above, we have rewritten our code so that the cost of the contractions associated with forming the genprops has been sped up by an order of magnitude. Thus is it now feasible to compute all the matrix elements required for the unpolarized and polarized GPDs as part of our program, as well as quantities such as the transversity distributions. The cost of these contractions are essentially the same as the cost of the inversions, so we simply scale the cost of inversions by a factor of two to arrive at the total cost per configuration. These are given in Table 3.

PROJECT III: Pion and Kaon Structure

A virtue of the distillation framework is that the same basic elements, namely the perambulators and the generalized perambulators, can be employed for a broad variety of physics projects. Thus for the study of pion structure, we need only compute the meson elementals of eqn. 3 that encode the pion interpolating operators, and then have all the components to obtain the pion two- and three-point functions both for the pion PDF and GPDs, and for the quark distribution amplitudes. However, for the case of the kaon we need to compute the additional generalized perambulators associated with the

Ens	Soln (c-s)	N_D	N_{t_i}	N_{sep}	N_b	N_{inv}	c-h/cfg	N_{cfg}	Tot (c-h)
E1	303	64	2	4	3	12,288	2,071	500	1,035K
E2	303	64	2	4	3	12,288	2,071	500	1,035K
E3	1,536	96	2	4	3	18,432	15,728	500	7,864K
E4	2,048	96	2	4	3	18,432	20,972	500	10,486K
TOTAL									20,421K

Table 3: The cost, in KNL core-hours, of computing the perambulators and generalized perambulators needed for studies of 3D hadron structure for each of the four ensembles of Table 1. The total number of inversions is as described in Table 2, noting an additional factor of 2 to account for the solutions from both the source t_i and sink t_f ; N_{sep} is the number of separations between the source and sink. Note that the cost of the matrix insertion of eqn. 6 represents a factor of two increase over the cost of the solutions.

insertion of the matrix elements in the strange-quark line. We observe only a small mass dependence, and therefore assume the cost of solution is that for the light quark. Since an important goal is the identification of differences between the properties of the kaon and the pion under the variation of the quark masses, we will employ the ensembles E1, E2 and E3 of Table 1.

Ens	Soln (c-s)	N_D	N_{t_i}	N_{sep}	N_b	N_{inv}	c-h/cfg	N_{cfg}	Tot (c-h)
E1	303	64	2	4	3	12,288	2,071	500	1,035K
E2	303	64	2	4	3	12,288	2,071	500	1,035K
E3	1,536	96	2	4	3	18,432	15,728	500	7,864K
TOTAL									9,934K

Table 4: The cost, in KNL core-hours, of computing the generalized perambulators associated with the insertion of matrix elements on a strange-quark line for the ensembles E1, E2 and E3 of Table 1.

Summary: We request **43.5M KNL-core-hours**, **7.43M Skylake-core-hours** and **0.78M RTX-GPU-hours**

Storage: The baryon elementals are the most expensive element of our calculation in terms of storage. Per configuration of the E3 lattice they require 250 GByte of storage, or 88 TByte for the full ensemble. We therefore request another 100 TByte of Tape storage, and 30 TByte of disk storage to facilitate 100 configurations of data of the largest ensemble to be on disk.

Readiness and Run Schedule

The software used in this proposal is that of USQCD, and in particular *Chroma*. A major stumbling block in starting our allocation this year has been deriving an efficient work flow for the computation of the gluonic elements using the RTX nodes at Jefferson Lab, and the SKX nodes at FNAL; this has now been solved somewhat effectively by computing the baryon elementals "on the fly" to obtain the required statistics for these matrix elements.

Data sharing and exclusive rights

We note that most of the data generated as part of this proposal comprises the correlators, the “perambulators”, “generalized perambulators”, and elementals. These are in general very specific to our projects rather than of general use.

References

- [1] Fritzsche H, Gell-Mann M and Leutwyler H 1973 *Phys. Lett.* **47B** 365–368
- [2] Politzer H D 1973 *Phys. Rev. Lett.* **30** 1346–1349 [,274(1973)]
- [3] Gross D J and Wilczek F 1973 *Phys. Rev. Lett.* **30** 1343–1346 [,271(1973)]
- [4] Wilson K G 1974 *Phys. Rev.* **D10** 2445–2459 [,45(1974); ,319(1974)]
- [5] Ji X 2013 *Phys. Rev. Lett.* **110** 262002 (*Preprint* 1305.1539)
- [6] Ji X 2014 *Sci. China Phys. Mech. Astron.* **57** 1407–1412 (*Preprint* 1404.6680)
- [7] Ma Y Q and Qiu J W 2018 *Phys. Rev.* **D98** 074021 (*Preprint* 1404.6860)
- [8] Liu K F 2016 *PoS LATTICE2015* 115 (*Preprint* 1603.07352)
- [9] Orginos K, Radyushkin A, Karpie J and Zafeiropoulos S 2017 *Phys. Rev.* **D96** 094503 (*Preprint* 1706.05373)
- [10] Chambers A J, Horsley R, Nakamura Y, Perlt H, Rakow P E L, Schierholz G, Schiller A, Somfleth K, Young R D and Zanotti J M 2017 *Phys. Rev. Lett.* **118** 242001 (*Preprint* 1703.01153)
- [11] Radyushkin A V 2017 *Phys. Rev.* **D96** 034025 (*Preprint* 1705.01488)
- [12] Ma Y Q and Qiu J W 2018 *Phys. Rev. Lett.* **120** 022003 (*Preprint* 1709.03018)
- [13] Karpie J, Orginos K and Zafeiropoulos S 2018 *JHEP* **11** 178 (*Preprint* 1807.10933)
- [14] Joó B, Karpie J, Orginos K, Radyushkin A, Richards D and Zafeiropoulos S 2019 *JHEP* **12** 081 (*Preprint* 1908.09771)
- [15] Del Debbio L, Giani T, Karpie J, Orginos K, Radyushkin A and Zafeiropoulos S 2021 *JHEP* **02** 138 (*Preprint* 2010.03996)
- [16] Egerer C, Edwards R G, Orginos K and Richards D G 2021 *Phys. Rev. D* **103** 034502 (*Preprint* 2009.10691)
- [17] Peardon M, Bulava J, Foley J, Morningstar C, Dudek J, Edwards R G, Joo B, Lin H W, Richards D G and Juge K J (Hadron Spectrum) 2009 *Phys. Rev. D* **80** 054506 (*Preprint* 0905.2160)
- [18] Bali G S, Lang B, Musch B U and Schäfer A 2016 *Phys. Rev. D* **93** 094515 (*Preprint* 1602.05525)
- [19] Joó B, Karpie J, Orginos K, Radyushkin A V, Richards D G, Sufian R S and Zafeiropoulos S 2019 *Phys. Rev.* **D100** 114512 (*Preprint* 1909.08517)
- [20] Balitsky I, Morris W and Radyushkin A 2019 (*Preprint* 1910.13963)

- [21] Sufian R S, Liu T and Paul A 2021 *Phys. Rev. D* **103** 036007 (*Preprint* 2012.01532)
- [22] Arrington J *et al.* 2021 (*Preprint* 2102.11788)
- [23] Romero E, Stathopoulos A and Orginos K 2020 *Journal of Computational Physics* **409** 109356 ISSN 0021-9991 URL <http://www.sciencedirect.com/science/article/pii/S0021999120301303>
- [24] Gambhir A S, Stathopoulos A and Orginos K 2017 *SIAM Journal on Scientific Computing* **39** A532–A558